

# Maximum mass of neutron stars and strange neutron-star cores

J.L. Zdunik and P. Haensel

N. Copernicus Astronomical Center, Polish Academy of Sciences, Bartycka 18, PL-00-716 Warszawa, Poland  
j1z@camk.edu.pl, haensel@camk.edu.pl

Received xxx Accepted xxx

## ABSTRACT

**Context.** Recent measurement of mass of PSR J1614-2230 rules out most of existing models of equation of state (EOS) of dense matter with high-density softening due to hyperonization, based on the recent hyperon-nucleon and hyperon-hyperon interactions, leading to a "hyperon puzzle".

**Aims.** We study a specific solution of "hyperon puzzle", consisting in replacing a too soft hyperon core by a sufficiently stiff quark core. In terms of the quark structure of the matter, one replaces a strangeness carrying baryon phase of confined quark triplets, some of them involving s quarks, by a quark plasma of deconfined u, d, and s quarks.

**Methods.** We construct an analytic approximation fitting very well modern EOSs of 2SC and CFL color superconducting phases of quark matter. Then, we use it to generate a continuum of EOSs of quark matter. This allows us for simulating continua of sequences of first-order phase transitions, at prescribed pressures, from hadronic matter to the 2SC, and then to the CFL state of color superconducting quark matter.

**Results.** We obtain constraints in the parameter space of the EOS of superconducting quark cores, EOS.Q, resulting from  $M_{\max} > 2 M_{\odot}$ . These constraints depend on the assumed EOS of baryon phase, EOS.B. We also derive constraints that would result from significantly higher measured masses. For  $2.4 M_{\odot}$  required stiffness of the CFL quark core should have been close to the causality limit, the density jump at the phase transition being very small.

**Conclusions.** Condition  $M_{\max} > 2 M_{\odot}$  puts strong constraints on the EOSs of the 2SC and CFL phases of quark matter. Density jumps at the phase transitions have to be sufficiently small and sound speeds in quark matter - sufficiently large. A strict condition of thermodynamic stability of quark phase results in the maximum mass of hybrid stars similar to that of purely baryon stars. Therefore, to get  $M_{\max} > 2 M_{\odot}$  for stable hybrid stars, both sufficiently strong additional hyperon repulsion at high density baryon matter *and* a sufficiently stiff EOS of quark matter would be needed. However, it is likely that the high density instability of quark matter (reconfinement of quark matter) indicates actually the inadequacy of the point-particle model of baryons in dense matter at  $\rho \gtrsim 5 \div 8 \rho_0$ .

**Key words.** dense matter – equation of state – stars: neutron

## 1. Introduction

The mass of PSR J1614-2230,  $1.97 \pm 0.04 M_{\odot}$  (Demorest et al., 2010), puts a constraint on the equation of state (EOS) of dense matter in neutron star (NS) cores. Namely, maximum allowable mass calculated using an acceptable EOS,  $M_{\max}(\text{EOS})$ , should be greater than  $2.0 M_{\odot}$ . This proves crucial importance of strong interactions in NS cores: their repulsive effect triples the value of  $M_{\max}$  compared to that obtained for non-interacting Fermi gas of neutrons,  $0.7 M_{\odot}$ .

Observational constraint  $M_{\max}(\text{EOS}) > 2.0 M_{\odot}$  is easy to satisfy if neutron star cores contain nucleons only, and realistic nuclear forces are used, and we get  $M_{\max}^{(N)}(\text{EOS}) > 2.0 M_{\odot}$  for many realistic nucleon interaction models (Lattimer, 2011). However, nuclear interaction models, consistent with experimental data on hypernuclei, predict the presence of hyperons at the densities exceeding  $2 - 3\rho_0$ , where normal nuclear density  $\rho_0 = 2.7 \times 10^{14} \text{ g cm}^{-3}$  (baryon number density  $n_0 = 0.16 \text{ fm}^{-3}$ ). Hyperonization of the matter implies a softening of the EOS, due to replacing of most energetic neutrons by massive, slowly moving hyperons. For realistic models of baryon interactions one gets then  $M_{\max}^{(B)} \lesssim 1.5 M_{\odot}$  (see, e.g. Burgio et al. 2011,

Vidana et al. 2011, Schulze & Rijken 2011, and references therein). Such a low  $M_{\max}$  is only marginally consistent with  $1.44 M_{\odot}$  of the Hulse-Taylor pulsar, but was contradicted already by  $1.67 \pm 0.04 M_{\odot}$  of PSR J1903-0327 (Champion et al. 2008; more precise value has been recently obtained by Freire et al. 2011).

Two solutions of the problem of a too low  $M_{\max}^{(B)}$  have been proposed after the discovery of a  $2 M_{\odot}$  pulsar.

**Strong hyperon repulsion at high density.** It has been suggested that adding a new component to the hyperon-hyperon interaction, important for  $\rho \gtrsim 5\rho_0$ , can stiffen the high-density EOS.B sufficiently to yield  $M_{\max} > 2.0 M_{\odot}$ . Repulsive interaction between baryons is supplied by the exchange of *vector mesons* (spin=1). Hyperon repulsion due to exchange of vector  $\phi$  mesons allows for  $M_{\max} > 2.0 M_{\odot}$ , without spoiling the agreement with nuclear and hypernuclear data (Bednarek et al., 2012, Weissenborn et al., 2012a,b, Lastowiecki et al., 2012). Dexheimer & Schramm (2008) give an earlier general discussion of vector-meson contribution to EOS. An additional increase of  $M_{\max}$  (above  $2.1 - 2.2 M_{\odot}$ ) can be obtained via some breaking of the SU(6) symmetry, usually applied to generate vector-meson - hyperon coupling constants from the nucleon one (Weissenborn et al., 2012b). Hyperon repulsion

Send offprint requests to: J.L. Zdunik

at high density is limited by the condition of thermodynamic stability (Bednarek et al., 2012).

**Stiff quark cores in NS.** From the point of view of quantum chromodynamics (QCD), appearance of hyperons in dense matter is associated with presence of the s-quarks, in addition to the u and d ones confined into nucleons. Some authors suggested that the the hyperon core in NS could actually be replaced by a core of the u-d-s quark matter (Baldo et al. 2006 and references in Schulze & Rijken 2011). Let us denote the EOS of the u-d-s quark matter by EOS.Q. To yield  $M_{\max} > 2.0 M_{\odot}$ , quark matter should have two important (necessary) features: (1) a significant *overall quark repulsion* resulting in a stiff EOS.Q; (2) a strong attraction in a particular channel resulting in a strong color superconductivity, needed to make the deconfined Q-phase energetically preferred over the confined B(baryon) one. After the announcement of the discovery of a 2  $M_{\odot}$  pulsar, several models of quark cores of NS (hybrid stars), having the properties necessary to yield  $M_{\max} > 2.0 M_{\odot}$ , have been proposed (Özel et al. 2010, Weissenborn et al. 2011, Klähn et al. 2011, Bonanno & Sedrakian 2012, Lastowiecki et al. 2012). The EOS of the hybrid baryon-quark (BQ) stars (EOS.BQ) was constructed using a two-phase model of B $\rightarrow$ Q transition, with different underlining theories of the B and Q phases.

There exist many models of color superconducting quark matter states (see, e.g., Alford et al. 2008). Two basic states are: two-flavor color superconducting (2SC) state and color flavor locked (CFL) superconducting state. In the 2SC state only light u and d quarks are paired. The 2SC state is predicted to be the ground state of quark matter at  $n_b \lesssim 4n_0$ . On the other hand, the CFL superconductor, in which all three flavors are paired, is predicted to prevail at high density,  $n_b \gtrsim 4n_0$ . Other superconducting states are also predicted (Alford et al., 2008), but they will not be considered here.

In the present paper we derive constraints on the EOS.BQ using an analytical description of EOS.Q. This allows us to consider a continuum of the EOS.Q models, or, for a given EOS.B, a continuum of the EOS.BQ models. As the other authors, we use a two-phase description of 1st order phase transitions (no mixed-phase state; neglecting possibility of a mixed-phase state does not influence much the value of  $M_{\max}$ , see, e.g., Alford et al. 2005). We also discuss thermodynamic stability of the Q phase in stiff quark cores and its impact on  $M_{\max}$  (this problem has been already mentioned in Lastowiecki et al. 2012).

EOSs of baryon matter, used in our work, are described in Sect.2. In Sect.3 we construct an analytic approximation of the EOS of quark matter, and we show that it gives a precise approximation of several existing models of color-superconducting quark cores in neutron stars. Our analytic approximation is then used to construct a continuum of EOS.Q, suitable for constructing an EOS.BQ with phase transitions at prescribed pressures, for a given EOS.B. In Sect.3.2 we construct continua of the EOS.BQ models, for two models of EOS.B: a soft one, significantly violating a 2.0  $M_{\odot}$  bound, and a stiff one, satisfying this bound. Constraints on EOS.Q, resulting from  $M_{\max}^{(BQ)} > 2 M_{\odot}$ , are derived in Sect.4. We then study, in Sect.5, the thermodynamic stability of a stiff high-density quark matter. Finally,

in Sect.6 we summarize and discuss our results, and point out the weak points of our models.

Preliminary results of our work were presented at the ERPM Pulsar Conference, Zielona Góra, Poland, 24th-27th April, 2012.

## 2. EOSs of baryon matter

There are two types of existing EOS.B, leading to  $M_{\max} < 2 M_{\odot}$  and  $M_{\max} > 2 M_{\odot}$ , respectively. They will be hereafter referred to as *soft baryon EOS* and *stiff baryon EOS*. We will select one EOS belonging to each of these two groups, and use them to illustrate the features characteristic of the two types of EOS.B.

### 2.1. Soft baryon EOS

Most of existing EOS.B yield  $M_{\max}^{(B)}$  significantly lower than 2  $M_{\odot}$ . For them replacing a soft hyperon core by a stiff quark one seems to be an only way of getting  $M_{\max} > 2 M_{\odot}$ <sup>1</sup>. As an example, we consider a very recent EOS.B of Schulze & Rijken (2011). This EOS was obtained using Brueckner-Hartree-Fock many-body approach, and a realistic up-to-date baryon interaction. In the nucleon sector, Argonne V<sub>18</sub> nucleon-nucleon potential (Wiringa et al., 1995) was used, supplemented with a phenomenological three-body force (Li et al., 2008). The hyperon-nucleon and hyperon-hyperon potentials were Nijmegen ESC08 (Rijken et al. 2010a,b). This EOS.B gives a low  $M_{\max}^{(B)} = 1.35 M_{\odot}$  (Schulze & Rijken 2011). It will be hereafter referred to as SR one.

### 2.2. Stiff baryon EOS

The number of EOS.B satisfying  $M_{\max} > 2 M_{\odot}$  started to increase steadily after the discovery of a 2  $M_{\odot}$  pulsar. We selected the BM165 EOS.B of Bednarek et al. (2012). This EOS was obtained using non-linear relativistic mean field model involving the baryon octet coupled to meson fields. The effective lagrangian includes, in addition to scalar and vector-meson terms, also terms involving hidden-strangeness scalar and vector-meson coupled to hyperons only. For this EOS.B we get  $M_{\max}^{(B)} = 2.04 M_{\odot}$ . It will be hereafter referred to as BM165.

## 3. Quark-matter cores and their EOS

We consider electrically neutral u-d-s quark matter in beta equilibrium and at  $T = 0$ . The baryon number density  $n_b = \frac{1}{3}(n_u + n_d + n_s)$ , the energy density is denoted  $\mathcal{E}$ , matter density  $\rho = \mathcal{E}/c^2$ , and baryon chemical potential  $\mu_b = d\mathcal{E}/dn_b$ . An important relation is  $n_b = dP/d\mu_b$ . The phase transitions under consideration are assumed to be 1st order ones. Therefore, they occur at a specific (sharp) value of pressure, and are accompanied by a density jump, from  $\rho_1$  to  $\rho_2$ . This is a good approximation for B $\rightarrow$ Q phase transition in cold dense matter, because the smoothing effect of the mixed B-Q state is small and can be neglected (Endo et al. 2006 and references therein). An im-

<sup>1</sup> It seems that such a possibility was first considered in (Baldo et al., 2006); we are grateful to David Blaschke for calling our attention to this paper.

portant parameter characterizing the density jump at the interface between the two phases is  $\lambda = \rho_2/\rho_1$ . Actually, as we have already mentioned in Sect.1, inclusion of a mixed-phase state does not change, to a very good approximation, the value of  $M_{\max}$  (Alford et al., 2005).

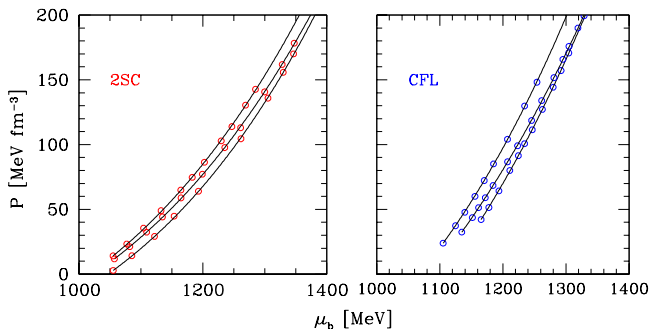


**Fig. 1.** (Online color) Calculated points of EOS of color superconducting quark matter in the  $P - \mu_b$  plane (Agrawal, 2010) and their approximation by our analytical formula. See the text for additional details.

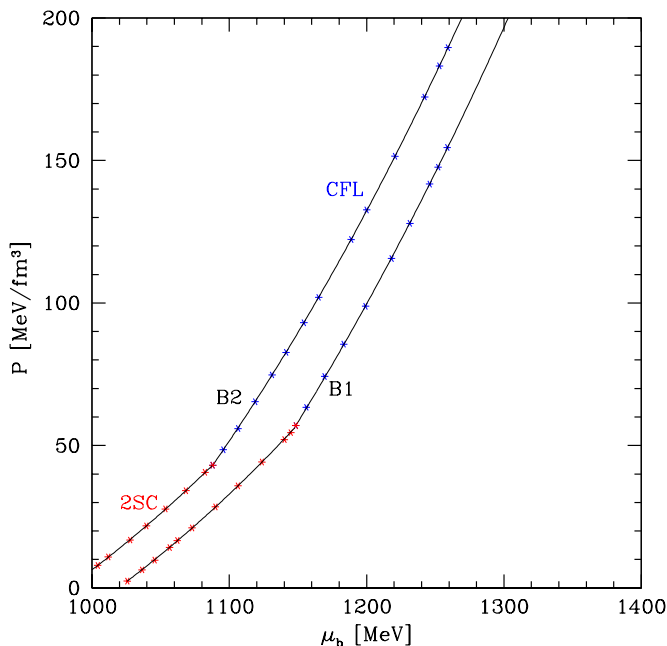


**Fig. 2.** (Online color) Calculated points of EOS of color superconducting quark matter in the  $P - \mu_b$  plane (Blaschke et al., 2010) and their approximation by our analytical formula. See the text for additional details.

### 3.1. Analytical approximation - 2SC and CFL phases

Our method is based on observation that starting from a simple linear formula one is able to get a rather precise analytic representation of modern EOS.  $Q(\mathcal{S})$  in a phase  $\mathcal{S} = 2SC, CFL$ , of color superconducting quark matter under

conditions prevailing in neutron star cores. In what follows, we will usually omit, for simplicity, the phase label  $\mathcal{S}$ .

Linear EOS ( $P$  being a linear function of  $\rho$ ) is characteristic of a simplest bag model of quark matter that assumes massless quarks, but it also holds with very high accuracy for more realistic bag model with massive s-quark (Zdunik, 2000).

Linear EOS is determined by three parameters:  $a$ ,  $\mathcal{E}_*$  and  $n_*$ , where  $a$  is square of sound velocity in the units of  $c$ , and  $\mathcal{E}_*$  and  $n_*$  are energy and baryon number density at zero pressure, respectively. We get then:

$$\begin{aligned} P(\mathcal{E}) &= a(\mathcal{E} - \mathcal{E}_*) \\ \mu(P) &= \mu_* \cdot \left[ 1 + \frac{1+a}{a} \frac{P}{\mathcal{E}_*} \right]^{a/(1+a)} \\ n(P) &= n_* \cdot \left[ 1 + \frac{1+a}{a} \frac{P}{\mathcal{E}_*} \right]^{1/(1+a)} = n_* \left( \frac{\mu}{\mu_*} \right)^{1/a} \end{aligned} \quad (1)$$

where  $\mu_* = \mathcal{E}_*/n_*$  is baryon chemical potential at zero pressure. The stiffness of the matter is described by the parameter  $a = dP/d\mathcal{E} = (v_{\text{sound}}/c)^2$ . Special cases of linear EOSs with  $a = 1$  and  $a = 1/3$  were recently considered by Chamel et al. (2012) in their study of exotic cores in neutron stars.

Numerical results for a quark matter EOS are usually given as points in the  $P - \mu_b$  plane (Agrawal, 2010, Blaschke et al., 2010). These variables are very convenient to study microscopic stability of matter and for determination of phase transition, which correspond to the crossing point of  $P(\mu)$  relations for different phases. The density jump at phase transition is described then by the change of the slope of  $P(\mu)$  function through the relations:  $n = dP/d\mu$  and  $\mathcal{E} = n\mu - P$  (see, e.g., Fig 2)

We assume that the linear EOS, Eq.(1), accurately describes quark matter cores in neutron stars, corresponding to baryon density range  $2n_0 \lesssim n_b \lesssim 10n_0$ . Let us stress, that the use of linear dependence, Eq.(1), is restricted to  $2n_0 - 10n_0$  (or  $300 \text{ MeV fm}^{-3} < \mathcal{E} < 1500 \text{ MeV fm}^{-3}$ , or  $30 \text{ MeV fm}^{-3} < P < 300 \text{ MeV fm}^{-3}$ ), and by no means is claimed to be valid outside the neutron-star core regime.

Let us introduce dimensionless quantities:  $\bar{n}_b \equiv n_b/n_*$  and  $\bar{\mu}_b \equiv \mu_b/\mu_*$ . We can then use Eq.(1) to get  $P$  as a function of  $\bar{\mu}_b$ ,

$$P = \frac{\mathcal{E}_*}{\nu} (\bar{\mu}_b^\nu - 1), \quad (2)$$

where  $\nu \equiv (1+a)/a$ . Then an analytical approximation for  $\bar{n}_b$  reads

$$\bar{n} = \frac{dP(\mu_b)}{d\mu_b} = \bar{\mu}_b^{\nu-1}. \quad (3)$$

Determination of the value of  $n_*$  deserves an additional comment. It can be taken from original numerical calculations if available. In not directly available, it can be calculated from the original plot of  $P^{(\text{calc})}(\mu_b)$  using  $n_* = (dP^{(\text{calc})}/d\mu_b)_{\mu_*}$ .

We now pass to specific cases of  $\mathcal{S} = 2SC, CFL$ . The least-squares fit method results in curves presented in Figs. 1, 2. This fit works very well and could be also checked by comparing values of  $n = dP/d\mu$  with exact results (if available, like in Agrawal 2010).

**2SC** In view of its intermediate-density range,  $2n_0 \lesssim n_b \lesssim 4n_0$ , the 2SC state is less important for  $M_{\max}$  than the high-density CFL state realized for  $n_b > 4n_0$ . However, as we will show, the softening due to the density jump

at the B-Q(2SC) transition has a significant indirect effect on the  $2 M_{\odot}$  constraint imposed on the EOS of the CFL phase. We considered two numerical EOS.Q(2SC)s, calculated by Agrawal (2010) and two of Blaschke et al. (2010). All these EOSs were calculated using the Nambu - Jona-Lasinio (NJL) model of quark matter and color superconductivity. The NJL model is a non-perturbative low-energy approximation to QCD. As seen in Figures 1, 2, our analytical formulae fit numerical results very precisely. It should be stressed, that these analytical formulae reproduce also very well numerically calculated points in the  $P - n_b$  plane, whenever these points are available, e.g., in Agrawal (2010). Our approximation in this case gives the value of parameter  $\nu = 4.1 \div 4.6$  which corresponds to  $a = 0.25 \div 0.33$ .

**CFL** The baryon density interval  $4n_0 \lesssim n_b \lesssim 10n_0$  is crucial for the value of  $M_{\max}$ . Therefore, it is the EOS in the CFL state which is decisive for the value of  $M_{\max}^{(\text{BQ})}$ . We considered five numerical EOS of CFL superconducting quark matter, three models from (Agrawal, 2010) and two models from (Blaschke et al., 2010). All of them were based on the NJL model. As we see in Figures 1, 2 our analytical formulae are very precise. Similarly as for the 2SC phase, these formulae reproduce also very well numerically calculated points in the  $P - n_b$  plane. The CFL phase is stiffer than the 2SC one: the values of  $a$  range within 0.3 and 0.4 ( $\nu = 3.5 \div 4.3$ ).

### 3.2. A family of analytical models of EOS.BQ

We generalize now discrete sets  $\{\mathcal{E}_{S^*}^i, a_S^i, n_{S^*}^i\}$  into a continuum of three-parameter models  $\{\mathcal{E}_{S^*}, a_S, n_{S^*}\}$ , within a region of parameter space determined by appropriate constraints on these parameters. We assume that  $0.2 < a < 0.8$ , while  $2n_0 < n < 10n_0$  and  $10 \text{ MeV fm}^{-3} < P < 300 \text{ MeV fm}^{-3}$ .

Having constructed a continuum of the EOS.Q(S) models we are able to simulate, for a given EOS.B, a sequence of phase transition  $\text{B} \rightarrow \text{Q}(2\text{SC}) \rightarrow \text{Q}(\text{CFL})$ .

**Transition from B to Q(2SC)** Assume that  $\text{B} \rightarrow \text{Q}(2\text{SC})$  takes place at  $P = P_1$ . Three parameters of an EOS.Q(2SC) taken from our family are then interrelated by two conditions at the  $\text{B} \rightarrow \text{Q}(2\text{SC})$  phase transition point : continuity of the baryon chemical potential, and continuity of the pressure,

$$\mu_b^{(\text{B})}(P_1) = \mu_b^{(2\text{SC})}(P_1), \quad P^{(\text{B})}(\mathcal{E}_1) = P^{(2\text{SC})}(\mathcal{E}_2). \quad (4)$$

Upper indices (B) and (2SC) refer to the baryon phase, and the 2SC quark phase, respectively. Now, let us fix the EOS of baryon matter, EOS.B. Models of the phase transition to the 2SC quark matter are then labeled by  $P_1 = P^{(\text{B})}(\mathcal{E}_1)$  and the relative density jump  $\lambda_{2\text{SC}} = \mathcal{E}_2/\mathcal{E}_1$ , with thermodynamical parameters  $(n_1, n_2, \mathcal{E}_1, \mathcal{E}_2)$  satisfying Equations (4). Here, the index 1 refers to the B phase, and 2 to the 2SC phase.

**Transition from Q(2SC) to Q(CFL)** Let us now choose the pressure at which the  $2\text{SC} \rightarrow \text{CFL}$  transition occurs,  $P = P_2$ . Using conditions of continuity of the pressure and of the baryon chemical potential at  $P = P_2$ , we obtain a one-parameter family  $\{\text{EOS.Q}(\text{CFL})\}$  attached to a specific EOS.Q(2SC) from the previously constructed  $\{\text{EOS.BQ}(2\text{SC})\}$  family. A continuous parameter within

$\{\text{EOS.Q}(\text{CFL})\}$  can be  $a_{\text{CFL}}$  or  $\lambda_{\text{CFL}}$ . This completes the second step in the procedure of constructing a general family  $\{\text{EOS.BQ}\}$  with  $\text{B} \rightarrow \text{Q}(2\text{SC}) \rightarrow \text{Q}(\text{CFL})$  phase transitions at prescribed pressures  $P_1$  and  $P_2$ , respectively.

In order to have a "reference one-phase quark core" we will also we consider EOS.BQ(CFL), with a phase transition from B directly to the CFL phase of quark matter, at pressure  $P_{\text{CFL}}$  and density  $\rho_{\text{CFL}}$ .

**Direct transition from B to Q(CFL) at  $P_{\text{CFL}}$ .** For  $P_1 < P_{\text{CFL}} < P_2$  this EOS can be either softer or stiffer than in the case of  $\text{B} \rightarrow 2\text{SC} \rightarrow \text{CFL}$ , depending on the softness of the hyperonic EOS. This is illustrated in Fig. 3 where the "middle" model of  $\text{B} \rightarrow 2\text{SC}$  transition (with  $\lambda_{2\text{SC}} = 1.15$ ) gives a mean stiffness similar to that of the hyperon (B) phase (i.e. pressures and densities at the bottom of CFL core are almost the same in both cases).

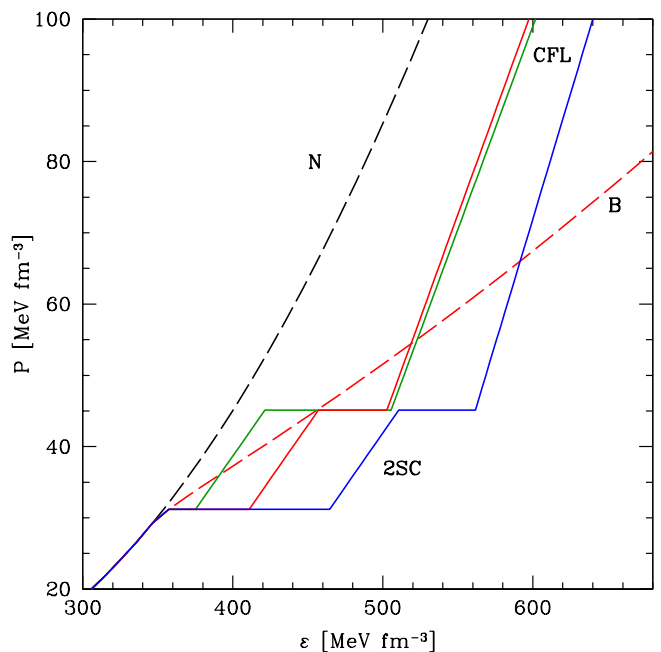


**Fig. 3.** (Online color) Examples of EOS.BQ from a continuum  $\{\text{EOS.BQ}\}$  emerging from a soft SR EOS. Hadronic EOSs are plotted as dashed lines: N - nucleon EOS; B - nucleons and hyperons. The phase transition  $\text{B} \rightarrow \text{Q}(2\text{SC})$  takes place at  $P_1 = 31 \text{ MeV fm}^{-3}$ , and  $\text{Q}(2\text{SC}) \rightarrow \text{Q}(\text{CFL})$  at  $P_2 = 45 \text{ MeV fm}^{-3}$ . The 2SC phase has  $a_{2\text{SC}} = 0.302$ . Three examples of  $\text{B} \rightarrow \text{Q}(2\text{SC}) \rightarrow \text{Q}(\text{CFL})$  are shown corresponding to following choices of  $\{\lambda_{2\text{SC}}, \lambda_{\text{CFL}}, a_{\text{CFL}}\}$ :  $\{1.05, 1.2, 0.57\}$ ,  $\{1.15, 1.1, 0.58\}$ ,  $\{1.3, 1.1, 0.7\}$ . In all these cases maximum mass is equal to  $2M_{\odot}$ , i.e., parameters  $\{\lambda_{2\text{SC}}, \lambda_{\text{CFL}}, a_{\text{CFL}}\}$  lie on the bounding curves in Fig. 7.

Several examples of EOS.BQ constructed following the procedure described above are shown in Figures 3, 4.

For two considered EOS.B, i.e. SR and BM165, we are using two different choices of transition pressures  $P_1$  and  $P_2$ . Here,  $P_1$  corresponds to the pressure at which in original models hyperons start to appear. For SR EOS  $P_1 \simeq 30 \text{ MeV fm}^{-3}$ , while for BM165 EOS  $P_1 \simeq 50 \text{ MeV fm}^{-3}$ . Thickness of the 2SC phase layer corresponds to  $\Delta P = P_2 -$

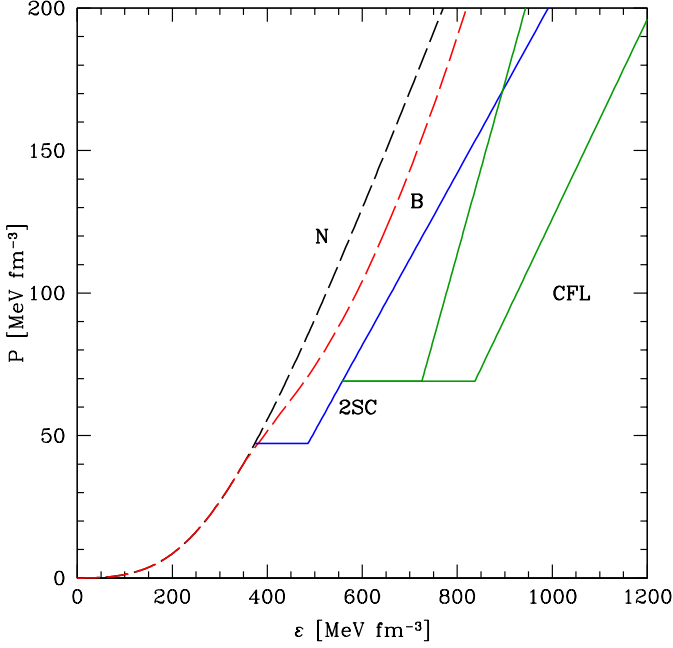


**Fig. 4.** (Online color) Examples of EOS.BQ from a continuum  $\{\text{EOS.BQ}\}$  emerging from a stiff MB165 EOS. Hadronic EOSs are plotted as dashed lines: N - nucleon EOS (black); B - nucleons and hyperons (red). The phase transition  $\text{B} \rightarrow \text{Q}(2\text{SC})$  takes place at  $P_1 = 47 \text{ MeV fm}^{-3}$ ,  $a_{2\text{SC}} = 0.302$  and  $\lambda_{2\text{SC}} = 1.3$ . EOS.Q(2SC) is plotted as a blue line. Two examples of  $\text{Q}(2\text{SC}) \rightarrow \text{Q}(\text{CFL})$  at  $P_2 = 69 \text{ MeV fm}^{-3}$  are shown, corresponding to a stiffer CFL phase ( $a_{\text{CFL}} = 0.6$ ,  $\lambda_{2\text{SC}} = 1.3$ ) and a softer one ( $a_{\text{CFL}} = 0.35$ ,  $\lambda_{2\text{SC}} = 1.5$ ). The EOS.Q(CFL)s are plotted as green solid lines.

$P_1 \approx 20 \text{ MeV fm}^{-3}$ . In both cases pressure  $P_1$  corresponds to  $n_b \approx 2n_0$ .

#### 4. Constraints on EOS.Q in the $a - \lambda$ plane

A 1st order phase transition in the neutron star core affects the EOS in two ways. First, it softens it because  $\lambda > 1$  implies some density range with  $dP/d\rho = 0$ . Second, a new phase is either stiffer or softer than the less dense phase, the stiffness of the quark phase being determined by  $a$ . The condition  $M_{\text{max}} > 2 M_{\odot}$  imposes therefore a condition in the  $a - \lambda$  plane. In what follows, we start with a case of a purely CFL quark core, and then we consider the quark core composed of an outer 2SC layer and an inner CFL core. Our results will be illustrated by examples presented in Figs 5-7. As in the preceding sections, we considered two EOS of baryon matter, a soft SR EOS, and a stiff BM165 EOS.

**Pure CFL core** We consider EOS.BQ(CFL), with quark core edge at  $P = P_{\text{CFL}}$ . We calculate a locus of points in the  $a_{\text{CFL}} - \lambda_{\text{CFL}}$  plane corresponding to  $M_{\text{max}} = 2 M_{\odot}$ . This locus is a line  $\lambda_{\text{max}}^{\text{CFL}}(a_{\text{CFL}})$  such that points  $(a, \lambda)$  below it generate Q-cores satisfying  $M_{\text{max}} > 2 M_{\odot}$ , while those above it violate this condition. We can alternatively call this locus line  $a_{\text{min}}^{\text{CFL}}(\lambda_{\text{CFL}})$ . Of course the location of lines  $a_{\text{CFL}} - \lambda_{\text{CFL}}$  depends on the value of pressure  $P_{\text{CFL}}$  (density

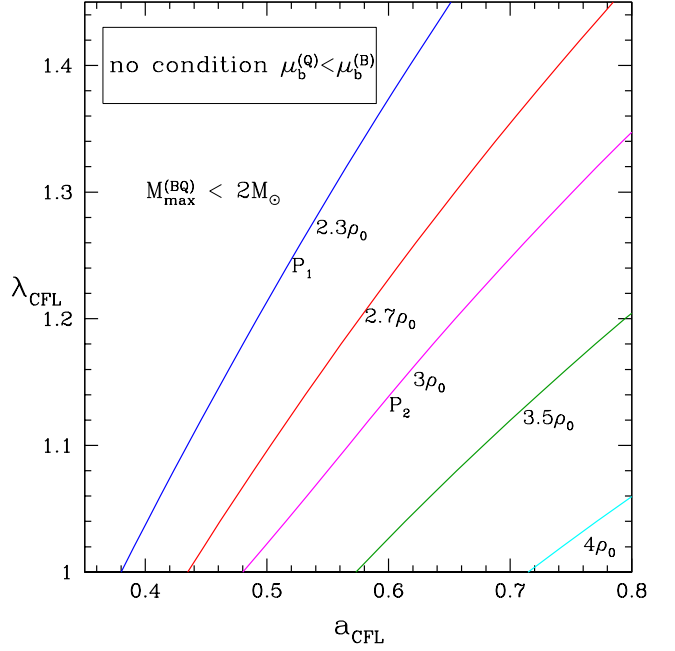


**Fig. 5.** (Color online) Constraints in the  $a - \lambda$  plane, resulting from  $M_{\text{max}} > 2 M_{\odot}$ , obtained assuming SR EOS of baryon matter, and for purely CFL cores (no 2SC layer) starting at  $\rho_{\text{CFL}} = 2.3\rho_0, \dots, 4.0\rho_0$ . Densities  $2.3\rho_0$  and  $3.0\rho_0$  correspond to  $P_1$  and  $P_2$  relevant for the boundaries of the 2SC layer in a 2SC+CFL core. Each line is an upper boundary of the region of  $(a_{\text{CFL}}, \lambda_{\text{CFL}})$  consistent with  $M_{\text{max}} > 2 M_{\odot}$ . These lines are labeled by the density  $\rho_{\text{CFL}}$  at which a direct transition  $\text{B} \rightarrow \text{Q}(\text{CFL})$  takes place.

$\rho_{\text{CFL}})$  at which phase transition to quark core (CFL) occurs. This dependence is presented in Fig. 5.

**2SC+CFL core, effect of a 2SC layer: general procedure** We replace an outer layer of the matter in the B phase containing hyperons (or a layer of the CFL core with pressures  $P_{\text{CFL}} < P < P_2$ ), by a layer of the 2SC phase. The effect of this additional layer of the 2SC phase depends on the value of  $P_{\text{CFL}}$ . If  $P_{\text{CFL}} = P_1$  we replace an outer layer of the CFL core by the quark matter in the 2SC phase. This will result in a softening of the quark core since 2SC phase is thought to be softer than the CFL one (due to a much smaller superfluid gap), and also because of an additional density jump  $\lambda_{2\text{SC}}$ . Even if  $\lambda_{2\text{SC}}$  is very close to one, we get  $\lambda_{\text{max}}^{\text{2SC+CFL}}(a) < \lambda_{\text{max}}^{\text{CFL}}(a)$ . However, the effect of 2SC phase on the value of  $\lambda_{\text{max}}^{\text{2SC+CFL}}$  is then rather small. With an increasing value of  $\lambda_{2\text{SC}}$ , the effect of softening gets stronger, and an allowed region of  $(a_{\text{CFL}}, \lambda_{\text{CFL}})$  gets smaller. In the limit of  $P_{\text{CFL}} = P_2$  we replace baryon matter by the 2SC phase and the net effect depends on the relative stiffness of these two phases (see Fig.3 and discussion at the end of Sect. 3.2).

**Stiff EOS.B, 2SC+CFL core** The loci  $a_{\text{min}}^{\text{CFL}}(\lambda_{\text{CFL}})$  are shown in Fig.6. Although the mass fraction contained in the 2SC layer is small, its effect on the size of the allowed  $(a_{\text{CFL}}, \lambda_{\text{CFL}})$  region is strong. For  $\lambda_{\text{CFL}} > 1.2$ , required  $a_{\text{CFL}}$  has to be significantly larger than the values obtained in (Blaschke et al., 2010, Agrawal, 2010). Simultaneously, at  $a_{\text{CFL}} \approx 0.5$  the density jump due to the  $2\text{SC} \rightarrow \text{CFL}$  tran-

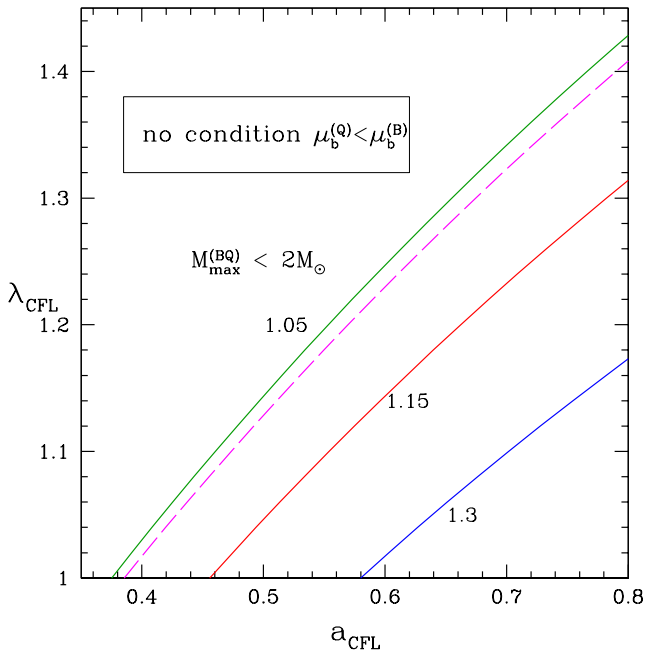


**Fig. 6.** (Color online) Constraints in the  $a - \lambda$  plane, resulting from  $M_{\max} > 2 M_{\odot}$ , obtained assuming BM165 EOS of baryon matter, and quark core starting at  $P_1 = 47 \text{ MeV fm}^{-3}$ . Each line is an upper boundary of the region of  $(a_{\text{CFL}}, \lambda_{\text{CFL}})$  consistent with  $M_{\max} > 2 M_{\odot}$ . Solid lines are obtained for quark cores composed of a 2SC layer ( $P_1 < P < P_2$ ) and a CFL core starting at  $P_2 = 69 \text{ MeV fm}^{-3}$ . These lines are labeled by the density jump at the B-2SC interface  $\lambda_{2\text{SC}} = 1.05, 1.15, 1.30$ . We used  $a_{2\text{SC}} = 0.3$  (Agrawal, 2010). Dashed line is obtained for purely CFL cores (no 2SC layer) starting at  $P_2$ .

sition is constrained to values significantly below the ones obtained in (Blaschke et al., 2010, Agrawal, 2010).

**Soft EOS.B, 2SC+CFL core** The loci  $a_{\min}^{\text{CFL}}(\lambda_{\text{CFL}})$  are shown in Fig. 7. Even for a very low density jump  $\lambda_{2\text{SC}} = 1.05$ , we obtain  $a_{\text{CFL}} > 0.4$ , which is rather stringent. In our case, the result obtained for  $\text{B} \rightarrow \text{Q}(\text{CFL})$  at  $P_{\text{CFL}} = P_2$  is very similar to that of  $\text{B} \rightarrow \text{Q}(2\text{SC}) \rightarrow \text{Q}(\text{CFL})$  with  $\lambda_{2\text{SC}} = 1.15$  (the dashed line is very close to the solid one).

## 5. Stability of quark cores and $M_{\max}$

Up to now, we did not consider the (thermodynamical) *stability* of a stiff quark core in a hybrid (BQ) star. A stiffening of the EOS is necessarily associated with the increase of the baryon chemical potential (see an example in Bednarek et al. 2012). In particular, it may lead to the thermodynamical instability of the stiff (Q) phase with respect to the re-conversion into the (B) one. This instability results from the violation, above a certain pressure, of the condition  $\mu_b^{(\text{Q})}(P) < \mu_b^{(\text{B})}(P)$ . Assuming a complete thermodynamical equilibrium, we are dealing with a first-order phase transition back to the (B) phase, that one can call *reconfinement* (cf., Lastowiecki et al. 2012). A corresponding EOS will be denoted  $\text{EOS.}\overline{\text{BQ}}$  and the  $M(R)$  branch based on this EOS will be labeled  $\overline{\text{BQ}}$ . Examples of the N,B,BQ and

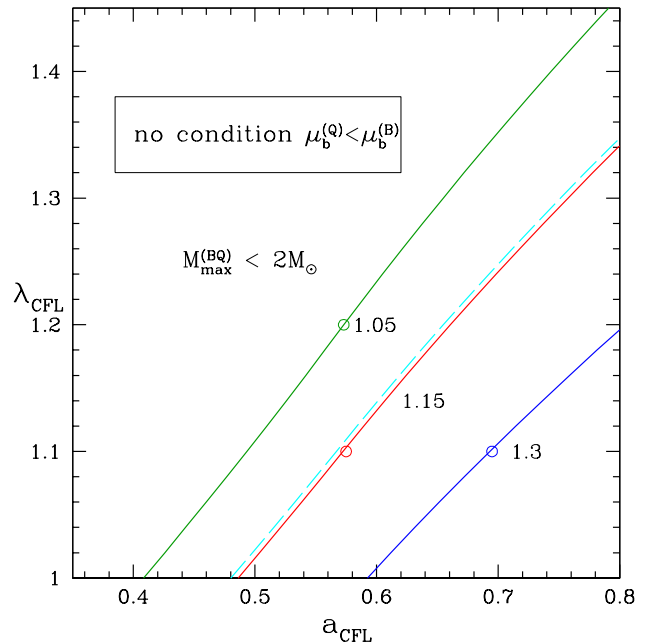


**Fig. 7.** (Color online) Constraints in the  $a - \lambda$  plane, resulting from  $M_{\max} > 2 M_{\odot}$ , obtained assuming SR EOS of baryon matter, and quark core starting at  $P_1 = 31 \text{ MeV fm}^{-3}$ . Each line is an upper boundary of the region of  $(a_{\text{CFL}}, \lambda_{\text{CFL}})$  consistent with  $M_{\max} > 2 M_{\odot}$ . Solid lines are obtained for quark cores composed of a 2SC layer ( $P_1 < P < P_2$ ) and a CFL core starting at  $P_2 = 45 \text{ MeV fm}^{-3}$ . These lines are labeled by the density jump at the B-2SC interface  $\lambda_{2\text{SC}} = 1.05, 1.15, 1.30$ . We used  $a_{2\text{SC}} = 0.3$  (Agrawal, 2010). Dashed line is obtained for purely CFL cores (no 2SC layer) starting at  $P_2 = 45 \text{ MeV fm}^{-3}$ . Open circles correspond to EOSs presented in Fig. 3.

$\overline{\text{BQ}}$  branches in the  $M - R$  plane, obtained for a soft SR EOS of baryon matter are presented in Fig. 8. The reconversion  $\text{Q} \rightarrow \text{B}$  strongly limits the size of the quark core in hybrid stars and results in the value of  $M_{\max}^{\overline{\text{BQ}}} \approx M_{\max}^{(\text{B})} = 1.35 M_{\odot}$  (Fig. 8)

For the BM165 EOS.B we get  $M_{\max}^{(\text{B})} = 2.04 M_{\odot}$ . Replacing hyperon cores by stiff quark ones can further increase the value of  $M_{\max}$ . An example is shown in Fig. 9, where we obtain  $M_{\max}^{(\text{BQ})} = 2.07 M_{\odot}$ . However, if complete thermodynamic equilibrium is imposed, the  $\text{Q} \rightarrow \text{B}$  transition back to the B phase takes place and one gets maximum allowable mass  $M_{\max}^{\overline{\text{BQ}}} \approx M_{\max}^{(\text{B})} = 2.04 M_{\odot}$ .

## 6. Summary, discussion, and conclusions

The existence of a  $2 M_{\odot}$  pulsar is a challenge for neutron star models with strangeness carrying cores. Strangeness is associated with s quark, either confined into hyperons or moving in a (deconfined) quark plasma.

The threshold density for the appearance of hyperons, predicted by realistic models of dense matter consistent with nuclear and hypernuclear data, is  $\sim 2\rho_0 - 3\rho_0$ . Realistic baryon interactions lead to  $M_{\max}$ , for neutron stars with hyperon cores starting at such density, that is significantly below  $M = 2.0 M_{\odot}$ . This contradiction can be removed

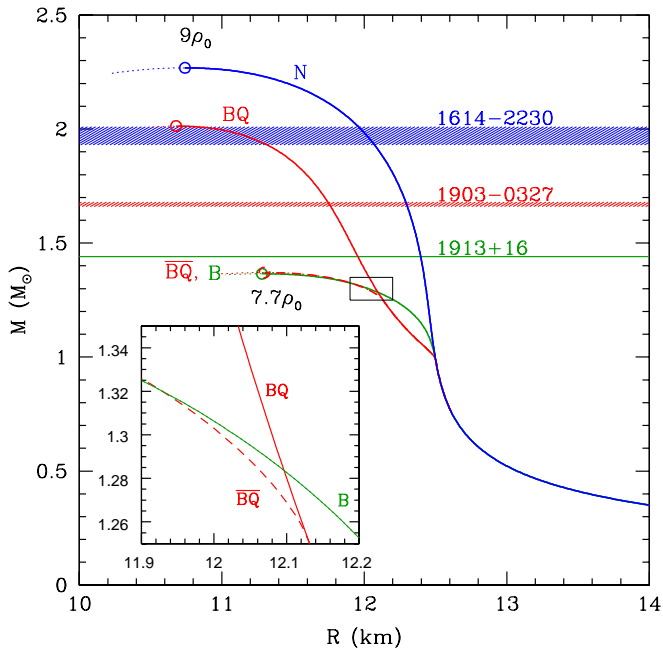


**Fig. 8.** (Color online) Mass  $M$  vs. radius  $R$  for non-rotating neutron star models calculated using different assumptions concerning structure of dense matter for  $\rho > 2\rho_0$ . Dotted segments of  $M(R)$  curves: configurations unstable with respect to small radial perturbations. N - nucleon matter, Argonne  $V_{18}$ +TBF nucleon interaction (Schulze & Rijken, 2011). B - baryon matter, EOS calculated using hyperon-nucleon and hyperon-hyperon potentials Nijmegen ESC08 (Rijken et al. 2010a,b). Open circles - configurations of maximum allowable mass, with central density given in the units of  $\rho_0$ . BQ - hybrid stars with quark cores, when condition  $\mu_b^{(Q)}(P) < \mu_b^{(B)}(P)$  is not imposed.  $\overline{BQ}$  - hybrid stars with stable quark cores, when condition  $\mu_b^{(Q)}(P) < \mu_b^{(B)}(P)$  is satisfied. Analytical EOS of quark matter in the CFL state with  $\rho_2 = 2.35\rho_0$ ,  $a_{\text{CFL}} = 0.5$ ,  $\lambda_{\text{CFL}} = 1.2$ . Enlarged rectangle: Vicinity of the high-density 1st order phase transition  $Q \rightarrow B$  (reconfinement).

due a hypothetical strong high-density repulsion acting between hyperons. As discussed in several papers, this strong high-density repulsion could result from the exchange of a vector meson  $\phi$  coupled only to hyperons.

However, it has also been considered that massive neutron stars could actually be hybrid stars with stiff quark-matter cores that allow for  $M > 2 M_{\odot}$ . Strong overall repulsion between quarks should be accompanied by a strong attraction (pairing) in a specific two-quark state, corresponding to a strong color superconductivity with a superfluid gap  $\sim 100$  MeV.

In the present paper we performed a general study of possibility for hybrid neutron stars with quark cores to reach  $M > 2 M_{\odot}$ . We considered a continuum of parameterized EOS of quark matter, including several existing models. This allowed us to consider general case of quark cores coexisting with baryonic matter at a prescribed pressure. We determined necessary features of baryon - quark-matter phase transition. First, the density at which first-order phase transition to quark phase occurs should be similar to the threshold density for hyperons,  $\sim 2\rho_0 - 3\rho_0$ .

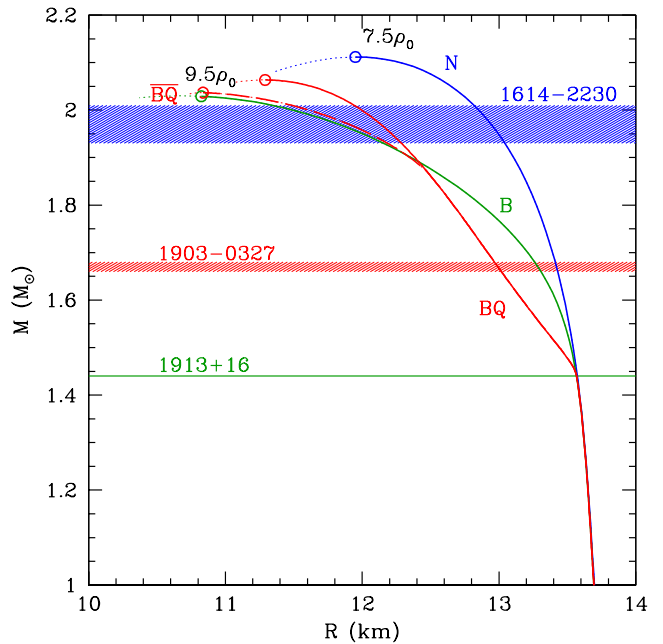


**Fig. 9.** (Color online) Same notations as in Fig.8, but for BM165 EOS of nucleon and baryon matter (Bednarek et al., 2012). Analytical EOS of quark matter and EOS.Q(CFL) with  $\rho_2 = 2.5\rho_0$ ,  $a_{\text{CFL}} = 0.5$ ,  $\lambda_{\text{CFL}} = 1.2$ .

Second the relative density jump at the baryon-quark matter phase transition should be below 30%. Third, quark matter should be sufficiently stiff, which can be expressed as a condition on the sound speed in quark plasma.

The measured  $2.0 M_{\odot}$  is actually a lower bound to a true  $M_{\text{max}} = M_{\text{max}}^{(\text{true})}$ . The upper bound, resulting the condition of speed of sound less than  $c$  combined with our confidence in the theoretical nucleon EOS for  $\rho < 2\rho_0$ , is  $3.0 M_{\odot}$  (see, e.g., Haensel et al. 2007, and references therein).  $M_{\text{max}}^{(\text{true})}$  lies therefore between  $2 M_{\odot}$  and  $3 M_{\odot}$ . Obviously, neutron star masses higher than  $2.0 M_{\odot}$  have to be contemplated. The question is how much higher? The mass of a "black widow" pulsar could be as high as  $2.4 M_{\odot}$ , albeit the present uncertainty is too large for this number to be used as an observational constraint (see, e.g., Lattimer 2011).

To discuss possibility of reaching masses significantly larger than  $2.0 M_{\odot}$  we plotted in Fig. 10 the bounding lines for  $M_{\text{max}}^{(\text{obs})} = 2.2 M_{\odot}$  and  $M_{\text{max}}^{(\text{obs})} = 2.4 M_{\odot}$ . As we see in Fig. 10, to fulfill condition  $M_{\text{max}}^{(\text{obs})} = 2.4 M_{\odot}$  we have to assume very stiff quark matter, quite close to the causality limit  $a = 1$ .

The situation becomes even more difficult if we require a strict stability of quark cores. As a result of high stiffness of quark matter, necessary for  $M_{\text{max}}^{(\text{obs})} > 2 M_{\odot}$  ( and a fortiori for higher lower bounds  $M_{\text{max}}^{(\text{obs})}$ ), the quark phase turns out to be unstable, beyond some pressure, with respect to hadronization. Assuming complete thermodynamic equilibrium, we get very similar  $M_{\text{max}}$  for the stars with hyperon and quark cores. Consequently, transition to quark matter could not yield  $M_{\text{max}} > 2 M_{\odot}$  if neutron stars with hyperonic cores had  $M_{\text{max}}^{(B)}$  (significantly) below  $2 M_{\odot}$ . This is

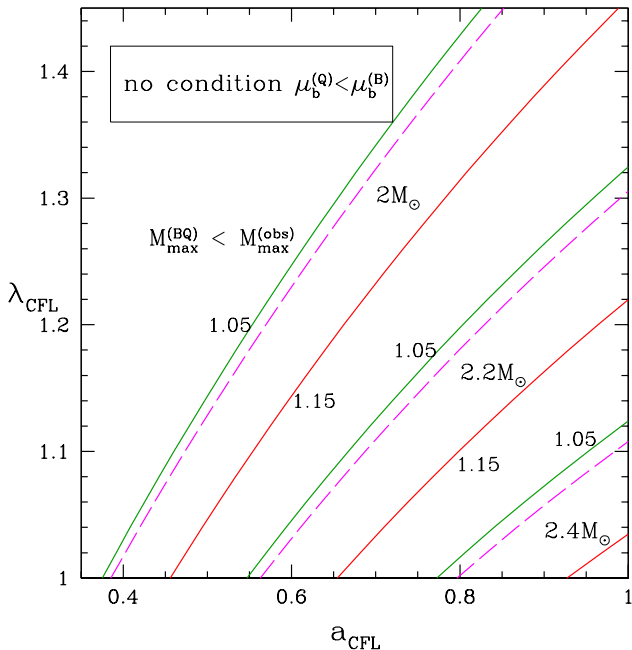


**Fig. 10.** (Color online) Constraints in the  $a - \lambda$  plane, resulting from 3 different values of maximum measured mass  $M_{\max}^{(\text{obs})} = 2.0 M_{\odot}, 2.2 M_{\odot}, 2.4 M_{\odot}$ . We assume BM165 EOS of baryon matter, and quark core starting at  $P_1 = 47 \text{ MeV fm}^{-3}$ . Each line is an upper boundary of the region of  $(a_{\text{CFL}}, \lambda_{\text{CFL}})$  consistent with  $M_{\max} > M_{\max}^{(\text{obs})}$ . Solid lines are obtained for purely CFL cores (no 2SC layer). Dashed lines are obtained for quark cores composed of a 2SC layer ( $P_1 < P < P_2$ ) and a CFL core starting at  $P_2 = 69 \text{ MeV fm}^{-3}$ . These lines are labeled by the density jump at the B-2SC interface  $\lambda_{2\text{SC}} = 1.05, 1.15$ . We used  $a_{2\text{SC}} = 0.3$  (Agrawal, 2010).

true also for  $M_{\max}^{(\text{obs})} > 2 M_{\odot}$ . Therefore, provided our picture of dense matter is valid, we find that a strong hyperon repulsion at high density is mandatory in general.

The high-density thermodynamic instability of the quark phase, and its consequences for  $M_{\max}$ , should be taken with a grain of salt. Our models of dense baryonic matter assume point particles. This assumption may be expected to break down at  $\rho \sim 5 \div 8\rho_0$ . Therefore, the "reconfinement" of the quark phase is, in our opinion, likely to indicate the inadequacy of point-particle baryonic phase model (see also Lastowiecki et al. 2012).

There is another weak point of the commonly used models of quark cores in neutron stars, characteristic also of the present paper: this is a two-phase approach, with each phase, baryon and quark one, treated using basically different descriptions. In principle, both phases and transition between them should have been treated using a unified approach based on the QCD, so that the influence of the dense medium on the baryon structure and baryon interactions are taken into account in a consistent way. Such approach is beyond the reach of the present day theory of dense matter. However, a phenomenological modeling of baryon structure in dense matter is possible, e.g., within a quark-meson coupling model (for references, see Whittenbury et al. 2012). More complete description of

neutron-star quark cores, going beyond the two-phase approximation, should hopefully be obtained in the future.

In this paper we were considering non-rotating configurations. Pulsar PSR J1614-2230 rotates with frequency  $f = 1/P = 317 \text{ Hz}$  and the effect for maximum mass is of the order of  $\simeq 0.01 M_{\odot}$  (Bednarek et al., 2012), much smaller than accuracy of mass determination. However it should be noted that for neutron star rotating with maximum observed frequency of 716 Hz the effect of rotation would be about five times larger.

*Acknowledgements.* We express our gratitude to David Blaschke and Rafał Lastowiecki for sharing their numerical results on the sound speed in quark matter. We are grateful to David Blaschke for reading the manuscript and calling our attention to several papers relevant to our work. We thank Nicolas Chamel for reading the manuscript and helpful remarks. This work was partially supported by the Polish MNiSW research grant no.N N203 512838.

## References

- Agrawal B.K. 2010, Phys. Rev. D 81, 023009  
 Alford, M., Braby, M., Paris, M., Reddy, S., 2005, ApJ, 629, 969  
 Alford, M.G., Schmitt, A., Rajagopal, K.I., Schaefer, T. 2008, Rev. Mod. Phys., 80, 1455  
 Baldo M., Burgio F., Schulze H.-J., 2006, in Superdense QCD Matter and Compact Stars (Springer), D. Blaschke and D. Sedrakian (eds.), p.113  
 Bednarek I., Haensel P., Zdunik J.L., Bejger M., Mańka R., 2012, A&A 543, 157  
 Blaschke D., Klähn T., Lastowiecki R., Sandin F. 2010, J. Phys. G: Nucl. Part. Phys 37, 094063  
 Bonanno, L., Sedrakian, A. 2012, A&A 539, A16  
 Burgio, G.F., Schulze, H.-J., Li, A., 2011, Phys Rev C, 83, 025804  
 Chamel, N., Fantina, A.F., Pearson, J.M., Gorieli, S., 2012, arXiv:1205.0983[nucl-th]  
 Champion D.J., et al., 2008, Science, 320, 1309  
 Demorest P.B., Pennucci T., Ransom S.M., Roberts M.S.E., Hessels J.W.T., 2010, Nature, 467, 1081  
 Dexheimer V., Schramm, S. 2008, ApJ, 683, 943  
 Endo T., Maruyama T., Chiba S., Tatsumi T., 2006, Prog. Theor. Phys. 115, 337  
 Freire P.C., et al., 2011, MNRAS, 412, 2763  
 Haensel, P., Potekhin, A.Y., Yakovlev, D.G. 2007, Neutron Stars 1. Equation of State and Structure (New York, Springer)  
 Klähn, T., Blaschke, D., Lastowiecki, R., 2011, arXiv:1111.6889v2[nucl-th] 30 Nov 2011  
 Lattimer, J.M., 2011, ASS, 336, 67  
 Li, Z.H., Lombardo, U., Schulze, H.-J., Zuo, W., 2008, Phys. Rev. C, 77, 034316  
 Lastowiecki, R., Blaschke, D., Grigorian, H., Typel, S., 2012, Acta Phys. Pol. B Proc. Suppl. 5, 535  
 Özel, F., Psaltis, D., Ransom, S., Demorest, P., Alford, M., 2010, ApJ Lett., 724, L199  
 Rijken, T., Nagels, M., Yamamoto, Y., 2010a, Nucl. Phys. A, 835, 160  
 Rijken, T., Nagels, M., Yamamoto, Y., 2010b, Prog. Theor. Phys. Suppl., 185, 14  
 Schulze H.-J., Rijken T. 2011, Phys. Rev. C 84, 035801  
 Vidana, I., Logoteta, D., Providencia, C., Bombaci, I., 2011, Europhys. Lett., 94, 11002  
 Weissenborn S., Sagert I., Pagliara G., Hempel M., Schaeffner-Bielich J. 2011, ApJ Lett. 740, L14  
 Weissenborn S., Chatterjee D., Schaeffner-Bielich J. 2012a, Nucl.Phys.A 881, 62  
 Weissenborn S., Chatterjee D., Schaeffner-Bielich J. 2012b, Phys Rev C, 85, 065802  
 Whittenbury, D.L., Carroll, J.D., Thomas, A.W., Tsushima, K., Stone, J.R. 2012, arXiv:1204.2614v1[nucl-th] 12 Apr 2012  
 Wiringa, R.B., Stoks, V.G.J., Schiavilla, R., 1995, Phys. Rev. C 51, 38  
 Zdunik, J.L., 2000, A&A 359, 311